

Numerical Characterization of the Mechanical Performance of SAC105 Tin-Silver-Copper Solder Interconnections After Aging



Mohammad A. Gharaibeh 

Department of Mechanical Engineering, Faculty of Engineering, The Hashemite University, Zarqa 13133, Jordan

Corresponding Author Email: mohammada_fa@hu.edu.jo

Copyright: ©2023 IETA. This article is published by IETA and is licensed under the CC BY 4.0 license (<http://creativecommons.org/licenses/by/4.0/>).

<https://doi.org/10.18280/acsm.470604>

ABSTRACT

Received: 5 October 2023

Revised: 18 November 2023

Accepted: 25 November 2023

Available online: 22 December 2023

Keywords:

SAC solders, isothermal aging, finite element method, solder creep

The evolution of mechanical properties and failure mechanisms in leadless solder interconnects, specifically 98.5Sn1.0Ag0.5Cu (SAC105), are continually influenced by isothermal aging and thermal loading over time. Accurate prediction of electronic assembly reliability necessitates the integration of these aging effects within the finite element analysis framework for solder thermal fatigue. This paper endeavors to elucidate the effects of pre-isothermal aging on the mechanical behavior of SAC105 interconnects under thermal cycling. Utilizing the finite element method coupled with material constitutive parameters from existing literature, the investigation examines two pivotal constitutive models—Anand and Garofalo. Creep behavior, characterized by Anand and Garofalo constants, is assimilated into the models to evaluate the aged SAC105's mechanical response during thermal cycling. Findings indicate that isothermal aging significantly alters the thermomechanical performance of SAC105 solder, particularly after brief aging periods, with diminishing impact over extended durations. Numerical analysis confirms the predominance of secondary creep in the mechanical response of SAC105, as opposed to isotropic hardening or viscoplasticity. Additionally, this study provides a comprehensive assessment of thermal fatigue in pre-aged solders, employing both strain-based and energy-based fatigue models. The insights reveal a reduced lifespan for aged solders compared to their unaged counterparts, with extended aging correlating with exacerbated thermal fatigue degradation. These outcomes furnish critical understanding for enhancing the reliability predictions of solder interconnects in electronic assemblies, post-isothermal aging.

1. INTRODUCTION

In the realm of microelectronics, significant advancements have been achieved, giving rise to devices that are not only compact but also boast heightened performance capabilities. This miniaturization trend poses challenges for reliability due to aging phenomena that can actuate failure mechanisms, necessitating a thorough investigation into the progression of such aging processes [1].

Investigations into the aging mechanisms of lead-free solders have revealed that thermal cycling and isothermal aging contribute to the evolution of their microstructure, which, in turn, influences their mechanical behavior and the mechanics of failure [2-4]. It has been documented that isothermal aging can precipitate a marked deterioration in the key mechanical properties of lead-free solder joints, encompassing the modulus of elasticity, as well as yield and tensile strengths [5, 6]. Moreover, alterations in the creep behavior of solders have been observed, with a significant increase in the creep strain rate, which poses detrimental effects on device reliability [7-9].

Empirical studies have provided evidence of these aging effects; for instance, Lee and Basaran [10] reported that isothermal aging at 100°C over a span of 1000 hours

detrimentally reduced the thermal fatigue life of plastic ball grid array (PBGA) packages. Zhang et al. [11] corroborated these findings in their scrutiny of wafer-level chip scale packages (WLCSP), and a multitude of corroborative studies have further reinforced these results [12-17].

The Finite Element Method (FEM) has been established as an invaluable tool in the assessment of fatigue life for electronic components, offering precise computation of stresses, deformations, and strains in solder interconnects [18-23]. For the fidelity of Finite Element Analysis (FEA) in predicting damage parameters, the accuracy of material property data is paramount.

Within the domain of reliability and fatigue analysis of solder joints, the foremost constitutive laws for creep in lead-free solders are identified as Garofalo's creep law [24]—often referred to as the hyperbolic sine creep equation—and the Anand model [25, 26]. These models are integral for accurate modeling and analysis, providing pivotal insights into solder joint behavior under various stress conditions [27-32].

It has been recognized that the pre-isothermal aging of lead-free solder joints necessitates careful consideration of aging time and temperature, which significantly influence the creep coefficients within Anand and Garofalo's models [33-35]. Accordingly, in the execution of finite element computations,

it is imperative that any variations in mechanical properties, specifically material constants, are meticulously incorporated. Such integration is essential to ensure the precision of damage projections, thereby enhancing the reliability assessment of electronic assemblies.

The discourse in preceding literature underscores the substantial role pre-aging exerts on the mechanical attributes of SAC (Sn-Ag-Cu) solder interconnects, influencing both their failure mechanics and thermal fatigue characteristics. This study is dedicated to examining the effect of pre-aging duration on the mechanical and creep responses of solder joints via finite element analysis. Furthermore, this investigation seeks to elucidate the correlation between pre-isothermal aging, the accrual of solder plastic strain, the entrapment of strain energy, and their collective impact on solder fatigue life.

For the purposes of this research, a comprehensive survey of reliable literature has been conducted to acquire the necessary mechanical and material parameters of solder alloys. Utilizing these properties, numerical analyses are performed, employing the Anand and Garofalo constitutive creep models to simulate the behavior of the solder. The findings of this study are anticipated to shed light on the effects of pre-isothermal aging on the mechanical behavior of solder and contribute to the enhancement of reliability assessments for electronic assemblies.

The structure of this paper is meticulously designed to unfold in a logical sequence, initiating with an in-depth exposé of the research problem and the variables under consideration. A thorough review of the Anand and Garofalo creep constitutive models follows. Subsequent to this, the finite element methodology employed in the current study is delineated, providing insights into the numerical simulations undertaken. The discourse progresses to an exhaustive analysis of the mechanical response of pre-aged SAC solders, scrutinizing the influence of pre-aging duration on their performance. This analysis is poised to offer invaluable insights that may bolster the reliability evaluations of electronic assemblies. In conclusion, the paper culminates with a synthesis of the research findings, encapsulating the essence of the study and postulating suggestions for prospective inquiries. These final remarks aim to underscore the study's contribution to the advancement of knowledge regarding the pre-isothermal aging of lead-free solder interconnects.

2. CREEP CONSTITUTIVE RELATIONS

Creep is designated as the mechanical event that is controlled by stress, temperature and loading rate and it is associated to the melting temperature of the metallic element and to the operating temperature as well. Normally, the onset of creep is triggered when the loading absolute temperature surpasses half, or sometimes 40%, of the melting point of the material [36]. In electronics, there are several common constitutive creep models that are widely used to simulate the mechanical creep of solder such as the Anand model.

2.1 Garofalo hyperbolic sine law

Garofalo's steady-state creep model [24], is regularly articulated by Garofalo-Arrhenius calculations to designate

the temperature-dependent steady-state, i.e., secondary, creep performance of the solder bonds, as:

$$\dot{\epsilon}_{cr} = A [\sinh(\alpha\sigma)]^\beta e^{\left(-\frac{Q}{RT}\right)} \quad (1)$$

where, T , σ , and $\dot{\epsilon}_{cr}$ and are the stress level, the absolute temperature (in Kelvin) and steady-state creep strain rate, respectively, and they are usually denoted as the loading parameters. The remaining material coefficients are the stress multiplier (α), the stress exponent (β), the pre-exponential factor (A) and (Q) is the activation energy while (R) is Boltzmann's constant.

2.2 The Anand model

The Anand model, is applied to simulate the hardening and viscoplastic deformations of metallic materials and it is designated by a set of constitutive relations [25, 26]. Largely, there are two central features of this model. First, the model necessitates no explicit yielding state and no loading or unloading criterion. Therefore, the permanent, strain is alleged to take place at all nonzero stress values. Second, the Anand model includes a single scalar as an internal variable as an interpretation for the internal isotropic material resistance to the plastic flow arisen by the initial state of the material. This crucial variable, symbolized by "s", is basically called the coefficient of deformation resistance. This "s" variable mostly characterizes the whole isotropic material resistance to the internal plastic flow in the material caused by the primary strengthening mechanisms such as, the dislocation movements or build-up, strengthening of the solid-solution as well as grain size/boundaries effects. Subsequently, the deformation resistance internal state variable (s) is directly and proportionally related to the equivalent stress.

As stated formerly, Anand law consists of a set of equations that consider the combined physical phenomena of loading temperature, loading or strain rate, strain hardening/softening, the strain rate history and the recovery of restoration process. Precisely, the inelastic strain rate ($\dot{\epsilon}_{in}$) in Anand model is written as:

$$\dot{\epsilon}_{in} = A \left[\sinh\left(\frac{\zeta\sigma}{s}\right) \right]^{1/m} e^{\left(-\frac{Q}{RT}\right)} \quad (2)$$

where, s is the internal variable; ζ and m are the stress multiplier as well as the strain rate sensitivity of stress, respectively. The rest of the variables (A, Q, R, T and σ) are defined as in Garofalo's equation presented in Eq. (1).

The internal variable is typically formalized via the evolution equation in a differential form ($\dot{s} = ds/dt$), as:

$$\dot{s} = \left\{ h_o \left(1 - \frac{s}{s^*} \right)^a \text{sign} \left(1 - \frac{s}{s^*} \right) \right\} \dot{\epsilon}_{in}, a \geq 1 \quad (3)$$

where, h_o is the hardening or softening parameter; a is the strain rate sensitivity of the hardening or softening and s^* is the saturation value of s and expressed by

$$s^* = \hat{s} \left[\frac{\dot{\epsilon}_{in}}{A} e^{\left(\frac{Q}{RT}\right)} \right]^n \quad (4)$$

where, n and \hat{s} are the strain rate sensitivity and coefficient of the saturated value of the deformation resistance, respectively. For the solder interconnects hardening behavior, Eq. (3) can be formulated as:

$$s = s^* - \left\{ (s^* - s_o)^{(1-a)} + (a-1) \left(\frac{h_o}{s^* a} \epsilon_{in} \right) \right\}^{1-a} \quad (5)$$

where, s_o is the deformation resistance initial value.

Consequently, nine coefficients ($s_o, Q/R, A, \zeta, m, h_o, a, \hat{s}$ and n) are necessary for the Anand model. These parameters are determined through robust nonlinear regressions of the measured stress-strain information obtained from tensile or shear tests, or from creep testing data. Actually, the Anand creep law is available in various FEA software packages like ANSYS, and it is normally accepted in simulating the creep behavior of different die attachments or solder interconnects in electronics.

3. DESCRIPTION OF THE PROBLEM

The primary objective of this article is to analyze the mechanical response of pre-isothermally aged SAC105 (98.5% Sn, 1.0% Ag, 0.5% Cu) solders under thermal cycling loading conditions using FEA computations. The aging process of lead-free solders is known to cause considerable changes in their mechanical as well as material properties. In the case of SAC solders, significant alterations in the elastic properties like Young's modulus and creep-related parameters, as in Anand model, are expected.

A previous research study [37] has conducted thorough experiments to obtain the material properties of SAC105 due to isothermal aging at a temperature of 100°C for different aging exposure periods of 0, 30, 60, 120 and 180 days (0, 1, 2, 4 and 6 months). The 0 days refers to the fact the aging process is not initiated yet (no aging). The stress-strain behavior of the aged SAC105 interconnects was then measured through tensile tests at three different strain rates (0.001, 0.0001, and 0.00001 per second) and five testing temperatures ranging from 25°C to 125°C. The resulting modulus of elasticity data, as well as yielding and UTS values, were extracted accordingly. Additionally, the nonlinear least square fits enabled the robust calculation of the Anand model parameters, which are detailed subsequently. Table 1 details the Young's modulus data of the pre-isothermally aged SAC105 solders.

In Anand modeling, it is apparent that Eq. (2), or the flow equation, is mathematically similar to Garofalo's law equation

(Eq. (1)), with some adaptations made to the internal variable (s). In fact, the stress multiplier α in Eq. (1) is equal to ζ/s in Eq. (2) (thus, $\alpha = \zeta/s$), and the exponent coefficients of the hyperbolic sine function are inter-related as $\beta = 1/m$.

Table 1. Young's modulus (in *GPa*) of SAC105 for different aging intervals (in days) and testing temperatures [37]

Temp. (°C)	0	30	60	120	180
25	36.0	24.1	21.2	19.5	19.4
50	32.5	22.3	18.7	16.5	16.5
75	28.4	21.1	17.9	15.8	16.1
100	25.0	19.7	16.8	15.1	15.2
125	21.2	17.7	16.1	14.8	14.7

However, it's important to note that Garofalo's law does not include the evolution of the hardening/softening process of Anand's model. In Garofalo's model, the s parameter is, in fact, constant, whereas in Anand's law, it is a variable that is responsible for the viscoplasticity behavior of the material. The remaining coefficients, like (A) and (Q/R), are indeed indistinguishable in both creep models.

In fact, it is credible to estimate the Anand model using Garofalo's law [38-40], which has been previously discussed in the framework of unleaded solder mechanical behavior. Specifically, when the deformation resistance variable (s) and the saturation value of stress (s^*) are equal, the solder steady-state plastic flow is activated. Therefore, the evolution equation of Anand's model (Eq. (3)) is skipped, and consequently the hardening process response is disregarded. Thus, the hardening parameter is reduced to zero ($h_o = 0$), and the loading rate sensitivity of the hardening process becomes a unity ($a = 1$). Additionally, the parameter for strain rate sensitivity of the saturation value (n) is zero. This results in the fact that the parameters s_o and \hat{s} are equal to the saturation value (s^*). Accordingly, the Anand model is estimated to Garofalo's hyperbolic sine law. This methodology is widely adopted in various literature works [41-44].

As mentioned previously, the key objective of this article is to examine the creep as well as the mechanical response of pre-isothermally aged unleaded solder interconnects when subjected to thermal cycling loading. This is achieved various creep models. The Anand model constants of the isothermally aged SAC105 solders used in this paper are summarized in Table 2, while the beforehand described procedure is employed to attain Garofalo's constants, which are detailed in Table 3.

Table 2. The 9 table coefficients for different aging intervals (in days) of the aged SAC105 [37]

Anand Coefficient	0	30	60	120	180
s_o	5.01	4.12	3.8	3.5	3.1
Q/R	8046	8046	8046	8046	8046
A	5535	6237	6881	7584	8165
ζ	8	8	8	8	8
m	0.69	0.62	0.57	0.53	0.51
h_o	119933	105656	100428	96467	91355
\hat{s}	42.75	37.49	33.2	29.5	27.1
n	0.0074	0.0062	0.0055	0.0049	0.0046
a	1.40	1.49	1.54	1.57	1.62

Table 3. The resulting approximate Garofalo's coefficients for the aged SAC105 considering various aging periods (days)

Garofalo's Coefficients	0	30	60	120	180
A	5535	6237	6881	7584	8165
α	0.1871	0.2134	0.2400	0.2712	0.2952
β	1.450	1.613	1.754	1.887	1.961
Q/R	8046	8046	8046	8046	8046

To effectively simulate and evaluate the behavior of aged SAC105 solders when exposed to thermal cycling loadings, the mechanical properties listed in this article (Tables 1-3) are applied during the (FEA) numerical computations. Specifically, systematic 3-dimensional nonlinear FEA simulations are carried out using the aforementioned literature-based material factors, including the elastic as well as creep constants.

This investigation aims to explore the effect of the pre-isothermal aging process on the mechanical response of the SAC105 solder balls when subjected to thermal loading conditions. This is accomplished by adopting two different models: Anand's viscoplasticity-based creep and Garofalo's secondary creep-based models. The specifics and the results of this examination are presented the following section of the finite element analysis procedure.

4. FINITE ELEMENT SIMULATIONS

The present study incorporated detailed explicit 3-dimensional nonlinear finite element analysis, using ANSYS Mechanical Pro 2021, to precisely calculate the stresses, strains, and the inelastic energy densities in the pre-isothermally aged unleaded SAC105 solder interconnects exposed to thermal cyclic loads. The model used for the analysis consisted of electronic package comprising a $76 \times 76 \times 1 \text{ mm}^3$ squared printed circuit board (PCB), a centrally located $13 \times 13 \times 1 \text{ mm}^3$ integrated circuit (IC) component and a 14×14 peripheral array of 98.5Sn1.0Ag0.5Cu (SAC105) ball grid array (BGA) joints with a total of 160 interconnects having a separating pitch distance of a 1 mm between any two adjacent joints. To decrease the FEA program solution time and CPU resources, only a symmetric quarter finite element model is studied. The boundary conditions (BCs) of this model are applied by imposing symmetric BCs on the cut planes of symmetry and by restraining the PCB at a particular node located at the board corner, to strict rigid body movements. The FE mesh is created by incorporating SOLID185 hexahedron 3-D ANSYS element during the mesh generation step resulting in a model of 22374 and 27570 elements and nodes, respectively. This model is presented in Figure 1.

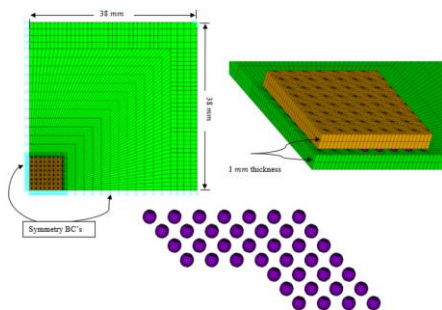


Figure 1. Finite element model details, Symmetry BC's, and the peripheral solder layout

For the material systems, linear elastic mechanical properties are employed for the board, the IC package, and the Cu pads, as detailed in Table 4.

Table 4. Elastic parameters of the PCB, Package and Copper used in the FEA simulations [38]

Parameter	Circuit Board	IC Component	Cu Pads
Young's modulus (GPa)	23.0	22.0	117.0
Poisson's ratio	0.16	0.3	0.33
Density (Kg/m ³)	3000	2000	8800
CTE (ppm/°C)	X, Y = 14.5 Z = 67.2	16.2	17.6

For the material modeling of the SAC105 interconnects, the previously discussed elastic (Young's modulus) and inelastic (creep parameters) properties are considered.

5. RESULTS AND DISCUSSIONS

5.1 Stress – strain ($\sigma - \epsilon$) charts

For accurate evaluations of the influence if the pre-isothermal aging of the unleaded solders, the present FEA is executed to simulate the response of the SAC105 interconnects due to temperature increase using a loading profile starting from 25°C to 200°C with a heating step of 25°C and rate 2.5°C per second. For this particular simulation, Anand's model is applied for the material constants of the lead-free SAC105 solders.

Accordingly, the solder temperature-induced shear stresses and shear strains are logged and then used to plot the stress-strain ($\sigma - \epsilon$) relationships for each aging condition as illustrated in Figure 2.

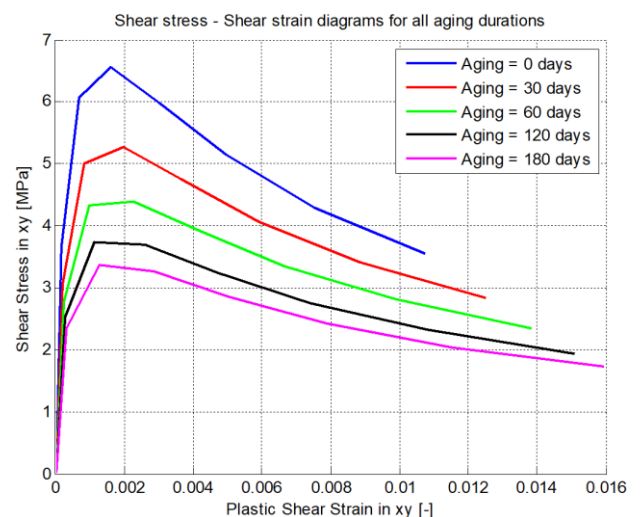


Figure 2. Shearing stress - strain relationships of the isothermally aged SAC105 due to temperature rise

It is evident from the $(\sigma - \epsilon)$ results that Young's modulus, yield stress, and UTS of the SAC105 solder decrease as the aging period extends. Nonetheless, the reduction in such mechanical properties is sizable in the shorter periods of aging (less than 2 months) and it becomes less significant for longer aging durations.

Additionally, as the SAC solder ages, the hardening behavior becomes less significant which can be attributed to the continuously decreasing value of the hardening coefficient in Anand's model (h_0) for the progressively aged SAC105 interconnect. Finally, it is also observable that longer aging eras yield to larger solder plastic strains. Meaning that the aged solders are more prone to plastic deformations and hence quicker failures.

5.2 Thermomechanical analysis

For further assessment of the mechanical response of the isothermally aged SAC105 solders, the current FEA model is utilized to accomplish nonlinear thermomechanical computations by applying five (5) complete thermal cycles according to the G-condition of (Joint Electron Devices Engineering Council) JEDEC standard [44] ($-40^{\circ}\text{C}/125^{\circ}\text{C}$ with 20 and 15 minutes of ramp and dwell times, respectively).

For this thermomechanical analysis, room temperature (25°C) is set as the zero-strain temperature and the large deformation option is turned-on throughout the simulations.

Both creep constitutive models, including Anand and Garofalo models, using the previously described material parameters are utilized in this simulation to inspect the differences between such creep laws on the mechanical behavior of the pre-aged SAC105 solder interconnects.

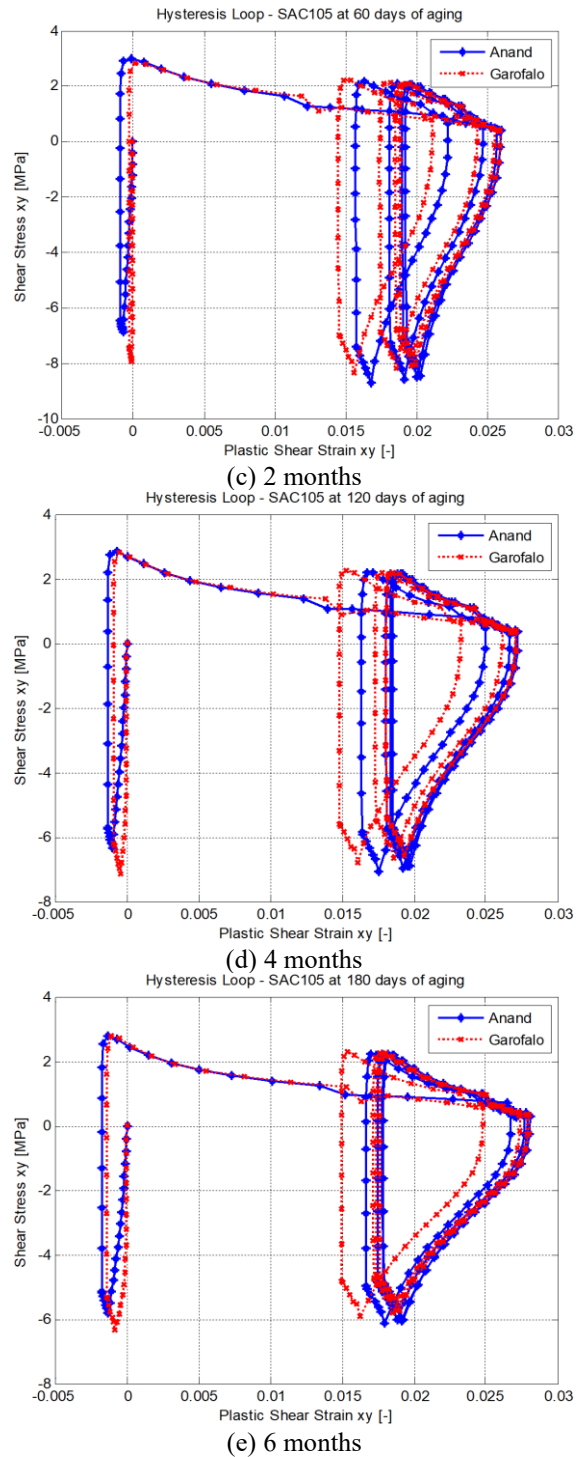
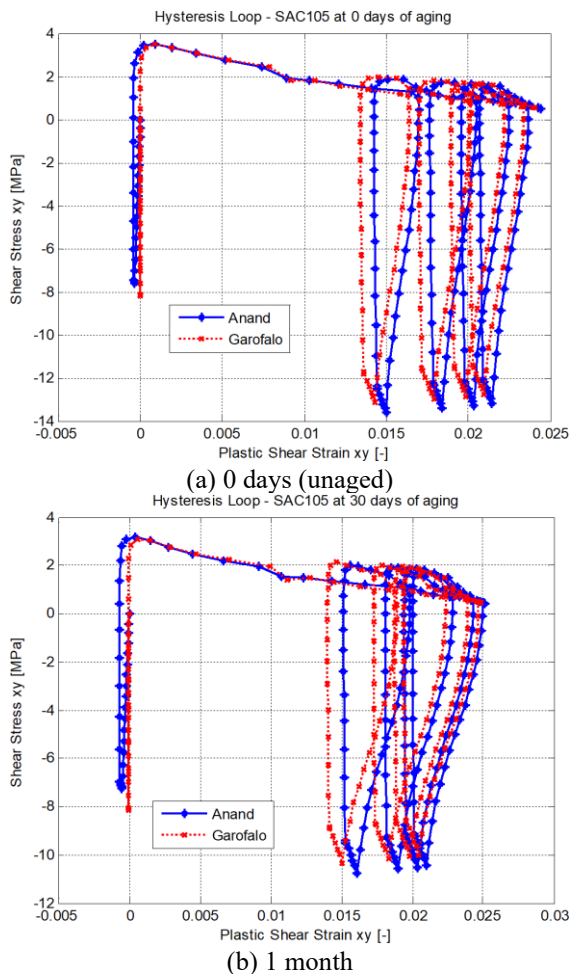


Figure 3. The hysteresis loops of the pre-aged SAC105 at various aging durations, using Anand and Garofalo creep laws

After the simulation is complete, the solder shear stresses, and shear strains are extracted and used to construct the hysteresis loop shown in Figure 3.

The stress and strain values here are taken at the node with the maximum stresses and strains. Care was taken that this node is far away from any stress singularities, i.e., material interfacing.

The results here show that before the aging process begins (0 days - Figure 3a), the hysteresis loop is very narrow, i.e. low plastic deformations, and the solder stresses are quite high (from -14 MPa to 2 MPa resulting in stress range of 16 MPa). However, as the aging process begins, the hysteresis loops

become wider, suggesting higher plastic deformations, while the stresses range is getting reduced. This means that the SAC105 solder after aging becomes more susceptible to plastic damage even at lower stress levels which makes them more prone to fatigue failures. Another observation is that the hysteresis loops from Anand's model are very similar to the loops resulting from Garofalo's steady-state creep model. This can be explained as for SAC105 lead-free interconnects, the steady-state creep is the main dominant creep distortions and the impact of the isotropic hardening and transient creep are, in fact, insignificant. Thus, Garofalo hyperbolic sine law can be feasibly used to demonstrate the creep response of the SAC105 solder joints.

Figure 4 presents the hysteresis loops of SAC105 load-free interconnect considering all aging conditions based on Garofalo's rule. The loop results here show that, again, the plastic shear strain for the unaged solder is small while the range of solder stress is significantly high. In other words, higher stress levels are required to start even little plastic deformations at this state. However, when the aging is in place, the solder plastic strain ranges become wider, and the stress range is considerably reduced. Meaning that a lower amount of stress is required to permanently deform the SAC105 solders. This is true as the aging period extends. Nonetheless, this becomes less dominant after a prolonged aging period, i.e., longer than 120 days. Specifically, the change in the plastic strain and stress ranges is insignificant. This is because the creep deformation consonants in both Anand and Garofalo models did not considerably change for such prolonger aging durations.

To sum up, the pre-isothermally aged SAC105 unleaded solders are expected to have extra severe degradations and thus shorter fatigue life than the unaged solders but the damage rate is varied for short and long periods of aging.

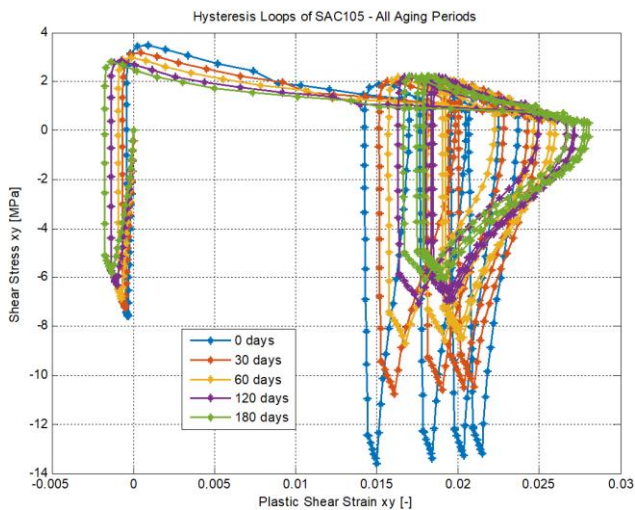


Figure 4. The FEA hysteresis loops of SAC105 considering various aging durations considering Garofalo creep relations

The lead-free solder joints' lifetime prediction models in literature can be categorized into two primary groups, namely, strain-based, and energy-based models. One of the widely accepted low cycle fatigue life calculation models for the strain-based models is Coffin-Manson's rule. The evaluation metric utilized in this law is the equivalent plastic strain. Additionally, an instance of the energy-based models is Darveaux's rule, which employs the inelastic strain energy density (SED_{in}). The current article examines these two

renowned fatigue life laws for the aged and unaged SAC105 interconnects.

From the previously described thermomechanical FEA computations, the equivalent plastic strain results as a function of the loading time as well as the accumulated equivalent plastic strains per cycle are shown in Figure 5. Apparently, the equivalent plastic strains are considerably higher when the aging process is applied. Additionally, the longer the isothermal aging period, the higher solder plastic strains are observed. Thus, shorter solder fatigue life is expected, according to Coffin-Manson's law.

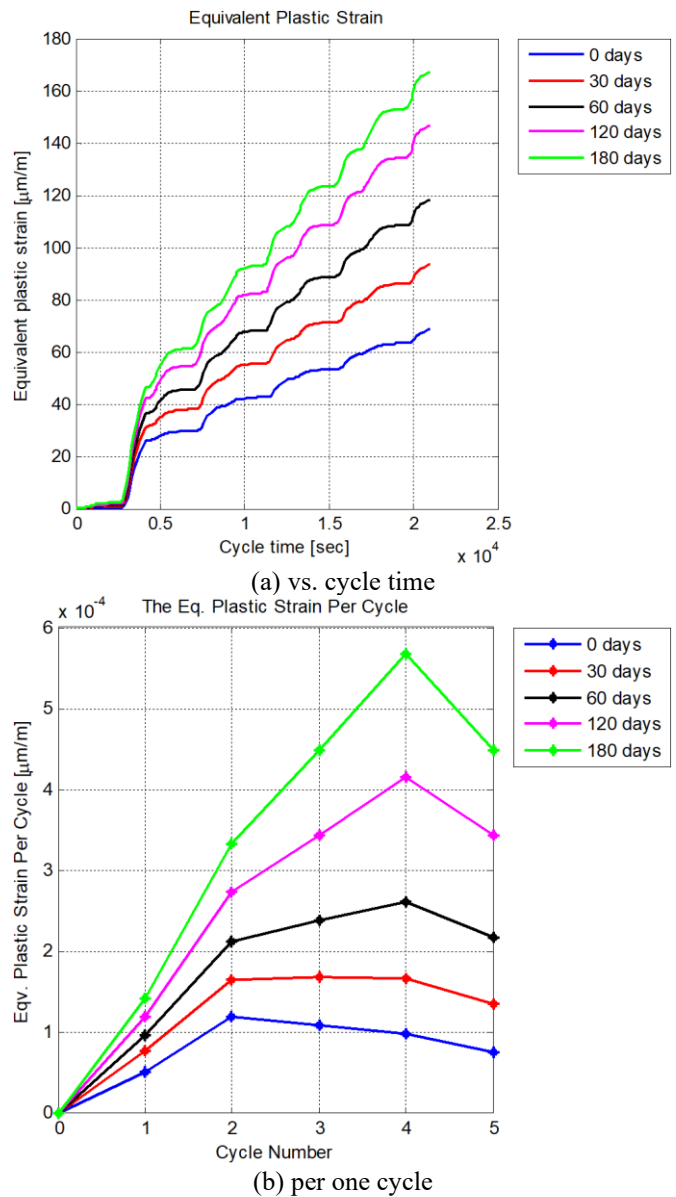


Figure 5. SAC105 max. equivalent plastic strains

In addition to the equivalent plastic strains, the SED_{in} , which is often denoted as the plastic work, results are evaluated. Figure 6 depicts the solder SED_{in} versus the loading period and the accumulated plastic work per cycle results as well. In fact, the longer the aging period is, the solder will exhibit larger inelastic strain energy densities. While the unaged SAC105 solder will have much lower accumulation of the inelastic SED. Therefore, the isothermal aging can lead to more plastic work accumulations and hence more solder damage and shorter fatigue life, per Darveaux's model evaluations. Furthermore, the plastic work accumulation in the

early aging stages (less than two months) is remarkably larger than that for longer aging periods (4 and 6 months). In fact, this was not clearly observed in the analysis of the equivalent plastic strains.

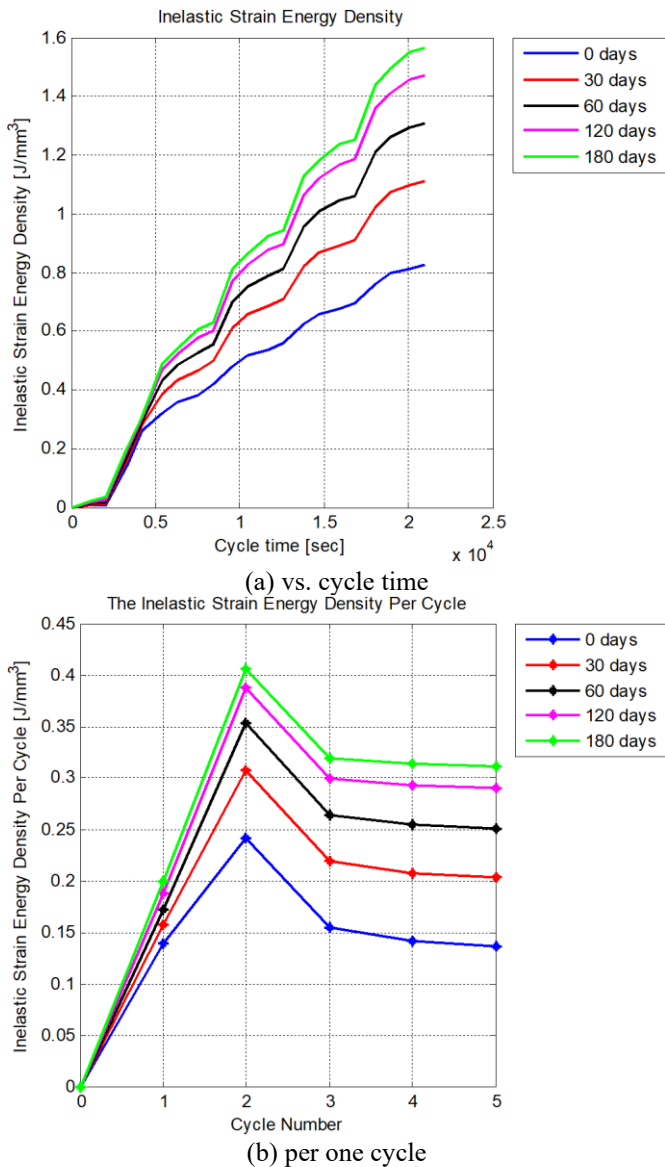


Figure 6. SAC105 SED_{in}

In summary, using energy-based fatigue life estimations, the longer aging durations leads to larger solder deteriorations and damage leading to shorter thermal fatigue life. However, the solder depreciation rate becomes less significant for the extended aging periods.

In conclusion, the isothermal aging of SAC105 solders could lead to significant solder damage and hence shorter thermal fatigue life, considering both strain-based as well as energy-based fatigue modeling criteria. However, the energy-based laws expect that this damage might become less effective as the pre-isothermal aging periods are considerably extended. To confirm such arguments, we highly recommend performing thermal fatigue life experiments on the aged SAC105 solders for better fatigue life quantification and accurate assessment of the engineering response of this lead-free interconnection.

6. CONCLUSIONS

This paper offered an extensive 3-D nonlinear finite element analysis to examine the influence of the pre-isothermal aging at 100°C, for aging periods ranging from one to six months, on the mechanical behavior and fatigue performance of SAC105 solders subjected to thermal cycling. The SAC105 properties, including elastic and creep coefficients, were obtained from dependable literature resources, and incorporated into the finite element analysis investigations. For solder material modeling, both Anand and Garofalo creep constitutive relations were employed. The FEA results demonstrated that the mechanical performance of aged solders is significantly impacted by the aging process and duration. The mechanical strength of the interconnections deteriorates comparatively with aging, with the rate of deterioration varying based on aging duration. The rate of deterioration is rapid for shorter aging periods, i.e., less than two months, and slows down for lengthy aging durations. Additionally, the numerical results showed that the SAC105 solder's mechanical response is mainly dominated by steady-state creep. The present research strongly recommends the correlations of the simulations results with future experimental work on the thermal fatigue life analysis of isothermally aged SAC105.

REFERENCES

- [1] Croes, K., Manca, J.V., De Ceuninck, W., De Schepper, L., Tielemans, L. (2001). Ageing and lifetime of electronic components studies by means of a high-resolution in-situ measurement technique. In *Ageing Studies and Lifetime Extension of Materials*, pp. 291-296. https://doi.org/10.1007/978-1-4615-1215-8_32
- [2] Maruf, M.A., Mazumder, G.R., Chakraborty, S., Suhling, J.C., Lall, P. (2023). Evolution in lead-free solder alloys subjected to both mechanical cycling and aging. *International Electronic Packaging Technical Conference and Exhibition, California, USA*, pp. V001T02A011. <https://doi.org/10.1115/IPACK2023-112023>
- [3] Ma, H., Suhling, J.C., Zhang, Y., Lall, P., Bozack, M.J. (2007). The influence of elevated temperature aging on reliability of lead free solder joints. In *2007 Proceedings 57th Electronic Components and Technology Conference*, pp. 653-668. <https://doi.org/10.1109/ECTC.2007.373867>
- [4] Gharaibeh, M.A. (2021). Optimization of dwell and ramp times for SAC305 solder thermal cycling fatigue life for testing and real-life applications. *Journal of Failure Analysis and Prevention*, 22: 276-285. <https://doi.org/10.1007/s11668-021-01290-9>
- [5] Zhang, Y., Cai, Z., Suhling, J.C., Lall, P., Bozack, M.J. (2009). The effects of SAC alloy composition on aging resistance and reliability. In *2009 59th Electronic Components and Technology Conference, San Diego, CA, USA*, pp. 370-389. <https://doi.org/10.1109/ECTC.2009.5074043>
- [6] Cai, Z., Zhang, Y., Suhling, J.C., Lall, P., Johnson, R.W., Bozack, M.J. (2010). Reduction of lead free solder aging effects using doped SAC alloys. In *2010 Proceedings 60th Electronic Components and Technology Conference (ECTC), Las Vegas, NV, USA*, pp. 1493-1511. <https://doi.org/10.1109/ECTC.2010.5490796>

- [7] Motalab, M., Cai, Z., Suhling, J.C., Zhang, J., Evans, J.L., Bozack, M.J., Lall, P. (2012). Improved predictions of lead free solder joint reliability that include aging effects. In 2012 IEEE 62nd Electronic Components and Technology Conference, San Diego, CA, USA, pp. 513-531. <https://doi.org/10.1109/ECTC.2012.6248879>
- [8] Mustafa, M., Cai, Z., Suhling, J.C., Lall, P. (2011). The effects of aging on the cyclic stress-strain behavior and hysteresis loop evolution of lead free solders. In 2011 IEEE 61st Electronic Components and Technology Conference (ECTC), Lake Buena Vista, FL, USA, pp. 927-939 <https://doi.org/10.1109/ECTC.2011.5898623>
- [9] Zhang, Y., Cai, Z., Suhling, J.C., Lall, P., Bozack, M.J. (2008). The effects of aging temperature on SAC solder joint material behavior and reliability. In 2008 58th Electronic Components and Technology Conference, Lake Buena Vista, FL, pp. 99-112. <https://doi.org/10.1109/ECTC.2008.4549956>
- [10] Lee, Y., Basaran, C. (2011). A Creep Model for Solder Alloys. *Journal of Electronic Packaging*, 133(4): 044501. <https://doi.org/10.1115/1.4005288>
- [11] Zhang, J., Hai, Z., Thirugnanasambandam, S., Evans, J.L., Bozack, M.J., Sesek, R., Zhang, Y., Suhling, J.C. (2012). Correlation of aging effects on creep rate and reliability in lead free solder joints. *SMTA Journal*, 25(3): 19-28.
- [12] Gharaibeh, M.A., Al-Oqla, F.M. (2023). Numerical evaluation of the mechanical response of Sn-Ag-Cu lead-free solders of various silver contents. *Soldering & Surface Mount Technology*, 35(5): 319-330. <https://doi.org/10.1108/SSMT-07-2023-0036>
- [13] Coyle, R., Parker, R., Henshall, G., Osterman, M., Smetana, J., Benedetto, E., Moore, D., Chang, G., Arnold, J., Lee, T.K. (2012). iNEMI Pb-free alloy characterization project report: Part IV-effect of isothermal preconditioning on thermal fatigue life. *Proceedings of SMTAI 2012*, pp. 376-389. https://thor.inemi.org/webdownload/Pres/SMTAI_2012/Pb-Free_Alloy/LF1-4_Coyle.pdf.
- [14] Coyle, R., McCormick, H., Osenbach, J., Read, P., Popowich, R., Fleming, D., Manock, J. (2011). Pb-free alloy silver content and thermal fatigue reliability of a large plastic ball grid array (PBGA) package. *SMTA Journal*, 24(1): 27-33.
- [15] Jong, W.R., Tsai, H.C., Huang, G.Z. (2009). The influences of temperature cycling parameters on the reliability of the solder joints in the high-density package assemblies by Taguchi Method. In 2009 4th International Microsystems, Packaging, Assembly and Circuits Technology Conference, Taipei, Taiwan, pp. 27-30. <https://doi.org/10.1109/IMPACT.2009.5382300>
- [16] Gharaibeh, M.A. (2021). A numerical analysis on the effect of point-support methods on the fatigue performance of thermally cycled electronic assemblies. *Microelectronics Reliability*, 127: 114419. <https://doi.org/10.1016/j.microrel.2021.114419>
- [17] Gharaibeh, M.A. (2022). Finite element analysis on the thermal fatigue life of full vs peripheral array packages. *Multidiscipline modeling in materials and structures*, 18(1): 87-94. <https://doi.org/10.1108/MMMS-08-2021-0148>
- [18] Gharaibeh, M. (2020). Experimental and numerical fatigue life assessment of SAC305 solders subjected to combined temperature and harmonic vibration loadings. *Soldering & Surface Mount Technology*, 32(3): 181-187. <https://doi.org/10.1108/SSMT-10-2019-0030>
- [19] Gharaibeh, M., Stewart, A.J., Su, Q.T., Pitarresi, J.M. (2018). Experimental and numerical investigations of the vibration reliability of BGA and LGA solder configurations and SAC105 and 63Sn37Pb solder alloys. *Soldering & Surface Mount Technology*, 31(2): 77-84. <https://doi.org/10.1108/SSMT-07-2018-0020>
- [20] Gharaibeh, M.A. (2021). A simulation-based study on the effect of package parameters on the random vibration behavior of electronic packages. *The European Physical Journal Plus*, 136(11): 1132. <https://doi.org/10.1140/epjp/s13360-021-02102-7>
- [21] Gharaibeh, M.A. (2022). Shock and impact reliability of electronic assemblies with perimeter vs full array layouts: A numerical comparative study. *Journal of the Mechanical Behavior of Materials*, 31(1): 535-545. <https://doi.org/10.1515/jmbm-2022-0058>
- [22] Gharaibeh, M.A., Pitarresi, J.M. (2022). A methodology to calculate the equivalent static loading for simulating electronic assemblies under impact. *Microelectronics Reliability*, 139: 114842. <https://doi.org/10.1016/j.microrel.2022.114842>
- [23] Gharaibeh, M. (2020). A numerical study on the effect of the fixation methods on the vibration fatigue of electronic packages. *Microelectronics Reliability*, 115: 113967. <https://doi.org/10.1016/j.microrel.2020.113967>
- [24] Garofalo, F. (1965). *Fundamentals of creep and creep-rupture in metals (Creep and creep rupture in metals and alloys, fundamental information for instruction and reference)*. New York, Macmillan Co., London, Collier-Macmillan, Ltd.
- [25] Anand, L. (1985). Constitutive equations for hot-working of metals. *International Journal of Plasticity*, 1(3): 213-231. [https://doi.org/10.1016/0749-6419\(85\)90004-X](https://doi.org/10.1016/0749-6419(85)90004-X)
- [26] Brown, S.B., Kim, K.H., Anand, L. (1989). An internal variable constitutive model for hot working of metals. *International Journal of Plasticity*, 5(2): 95-130. [https://doi.org/10.1016/0749-6419\(89\)90025-9](https://doi.org/10.1016/0749-6419(89)90025-9)
- [27] Syed, A. (2006). Updated life prediction models for solder joints with removal of modeling assumptions and effect of constitutive equations. In *EuroSime 2006-7th International Conference on Thermal, Mechanical and Multiphysics Simulation and Experiments in Micro-Electronics and Micro-Systems*, Como, Italy, pp. 1-9. <https://doi.org/10.1109/ESIME.2006.1644010>
- [28] Schubert, A., Dudek, R., Auerswald, E., Gollhardt, A., Michel, B., Reichl, H. (2003). Fatigue life models for SnAgCu and SnPb solder joints evaluated by experiments and simulation. In *Electronic Components and Technology Conference*, New Orleans, LA, USA, pp. 603-610. <https://doi.org/10.1109/ECTC.2003.1216343>
- [29] Gharaibeh, M.A., Wilde, J. (2023). Applying Anand versus Garofalo creep constitutive models for simulating sintered silver die attachments in power electronics. *The Journal of Strain Analysis for Engineering Design*. <https://doi.org/10.1177/03093247231190449>
- [30] Mukherjee, S., Nuhi, M., Dasgupta, A., Modarres, M. (2016). Creep constitutive models suitable for solder alloys in electronic assemblies. *Journal of electronic packaging*, 138(3): 030801. <https://doi.org/10.1115/1.4033375>

- [31] Knecht, S., Fox, L.R. (1990). Constitutive relation and creep-fatigue life model for eutectic tin-lead solder. *IEEE Transactions on Components, Hybrids, and Manufacturing Technology*, 13(2): 424-433. <https://doi.org/10.1109/33.56179>
- [32] Ma, H. (2009). Constitutive models of creep for lead-free solders. *Journal of Materials Science*, 44: 3841-3851. <https://doi.org/10.1007/s10853-009-3521-9>
- [33] Chen, G., Zhao, X., Wu, H. (2017). A critical review of constitutive models for solders in electronic packaging. *Advances in Mechanical Engineering*, 9(8): 1687814017714976. <https://doi.org/10.1177/1687814017714976>
- [34] Motalab, M., Mustafa, M., Suhling, J.C., Zhang, J., Evans, J., Bozack, M.J., Lall, P. (2013). Correlation of reliability models including aging effects with thermal cycling reliability data. In 2013 IEEE 63rd Electronic Components and Technology Conference, Las Vegas, NV, USA, pp. 986-1004. <https://doi.org/10.1109/ECTC.2013.6575694>
- [35] Motalab, M. (2013). A constitutive model for lead free solder including aging effects and its application to microelectronic packaging. Doctoral dissertation, Auburn University.
- [36] Dieter, G.E., Bacon, D. (1976). *Mechanical Metallurgy*. New York: McGraw-hill.
- [37] Lall, P., Yadav, V., Suhling, J., Locker, D. (2022). Evolution of Anand Parameters for Thermally Aged Sn-Ag-Cu Lead-Free Alloys at Low Operating Temperature. *Journal of Electronic Packaging*, 144(2): 021116. <https://doi.org/10.1115/1.4053764>
- [38] Gharaibeh, M.A. (2023). Nonlinear finite element simulations on the mechanical response of the isothermally aged lead-free solders. *Proceedings of the Institution of Mechanical Engineers, Part L: Journal of Materials: Design and Applications*, 237(11): 2421-2431. <https://doi.org/10.1177/14644207231179564>
- [39] Wiese, S., Feustel, F., Rzepka, S., Meusel, E. (1998). Experimental characterization of material properties of 63Sn37Pb flip chip solder joints. *MRS Online Proceedings Library (OPL)*, 515: 233. <https://doi.org/10.1557/PROC-515-233>
- [40] Fusaro, J.M., Darveaux, R. (1997). Reliability of copper baseplate high current power modules. *The International Journal of Microcircuits and Electronic Packaging*, 20(2): 81-88.
- [41] Wilde, J., Becker, K., Thoben, M., Blum, W., Jupitz, T., Wang, G., Cheng, Z. N. (2000). Rate dependent constitutive relations based on Anand model for 92.5 Pb5Sn2. 5Ag solder. *IEEE Transactions on Advanced Packaging*, 23(3): 408-414. <https://doi.org/10.1109/6040.861554>
- [42] Wang, G.Z., Cheng, Z.N., Becker, K., Wilde, J. (2001). Applying Anand model to represent the viscoplastic deformation behavior of solder alloys. *Journal of Electronic Packaging*, 123(3): 247-253. <https://doi.org/10.1115/1.1371781>
- [43] Cheng, Z.N., Wang, G.Z., Chen, L., Wilde, J., Becker, K. (2000). Viscoplastic Anand model for solder alloys and its application. *Soldering & Surface Mount Technology*, 12(2): 31-36. <https://doi.org/10.1108/09540910010331428>
- [44] JEDEC. (2009). Temperature cycling, In: JESD22-A104D; 2009. JEDEC solid state technology association. <https://www.jedec.org/sites/default/files/docs/22a104d.pdf>